

DESY 08-074
 LPSC 08-070

Modern Physics Letters A
 © World Scientific Publishing Company

Review of factorization breaking in diffractive photoproduction of dijets

MICHAEL KLASSEN

*Laboratoire de Physique Subatomique et de Cosmologie, Université Joseph Fourier /
 CNRS-IN2P3 / INPG, 53 Avenue des Martyrs, F-38026 Grenoble, France
 klasen@lpsc.in2p3.fr*

GUSTAV KRAMER

*II. Institut für Theoretische Physik, Universität Hamburg, Luruper Chaussee 149,
 D-22761 Hamburg, Germany*

Received (Day Month Year)
 Revised (Day Month Year)

After the final analyses of the H1 and ZEUS collaborations for the diffractive photoproduction of dijets have appeared, we have recalculated these cross sections in next-to-leading order (NLO) of perturbative QCD to see whether they can be interpreted consistently. The results of these calculations are compared to the data of both collaborations. We find that at NLO the cross sections disagree with the data, showing that factorization breaking occurs at this order. If direct and resolved contributions are both suppressed by the same amount, the global suppression factor depends on the transverse-energy cut and is 0.42 for the H1 and 0.71 for the ZEUS analysis. However, by suppressing only the resolved contribution by a factor of approximately three, also reasonably good agreement with all the data is found. The size of the factorization breaking effects for resolved photons agrees with absorptive-model predictions.

Keywords: Perturbative QCD; factorization; Regge theory; jet production.

12.38.Bx; 12.39.St; 12.40.Nn; 13.87.Ce.

1. Introduction

It is well known that at high-energy colliders such as the ep collider HERA at DESY and the $p\bar{p}$ collider Tevatron at Fermilab, a large fraction of the observed events are diffractive. These events are defined experimentally by the presence of a forward-going hadronic system Y with four-momentum p_Y , low mass M_Y (typically a proton that remained intact or a proton plus low-lying nucleon resonances), small four-momentum transfer $t = (P - p_Y)^2$, and small longitudinal-momentum transfer $x_{\mathbb{P}} = q(P - p_Y)/(qP)$ from the incoming proton with four momentum P to the central hadronic system X (see Fig. 1 for the case of $ep \rightarrow eXY$). Experimentally, a large rapidity gap separates the hadronic system X with invariant mass M_X from the final-state system Y with invariant mass M_Y .

Theoretically, diffractive interactions are described in the framework of Regge

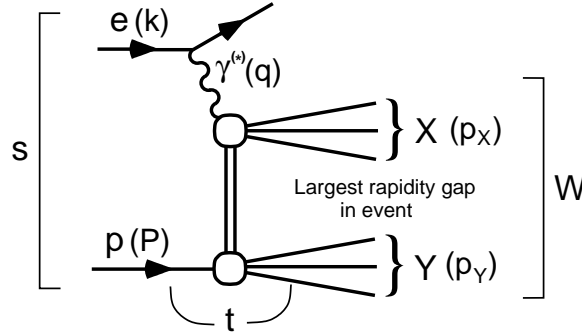
2 *M. Klasen, G. Kramer*


Fig. 1. Diffractive scattering process $ep \rightarrow eXY$, where the hadronic systems X and Y are separated by the largest rapidity gap in the final state.

theory¹ as the exchange of a trajectory with vacuum quantum numbers, the pomeron (P) trajectory. Then the object exchanged between the systems X and Y , as indicated in Fig. 1, is the pomeron (or additional lower-lying Regge poles), and the upper vertex of the process $eP \rightarrow eX$ can be interpreted as deep-inelastic scattering (DIS) on the pomeron target for the case that the virtuality of the exchanged photon $Q^2 = -q^2$ is sufficiently large. In analogy to DIS on a proton target, $ep \rightarrow eX$, the cross section for the process $eP \rightarrow eX$ in the DIS region can be expressed as the convolution of partonic cross sections and universal parton distribution functions (PDFs) of the pomeron. The partonic cross sections are the same as for DIS ep scattering. Usually these pomeron PDFs are multiplied with vertex functions for the lower vertex in Fig. 1, yielding the diffractive parton distribution functions (DPDFs). The Q^2 -evolution of the DPDFs is calculated with the usual DGLAP² evolution equations known from $ep \rightarrow eX$ DIS. Except for their evolution with Q^2 , the DPDFs can not be calculated in the framework of perturbative QCD and must be determined from experiment. Such DPDFs^{3,4,5,6} have been obtained from the HERA inclusive measurements of the diffractive structure function F_2^D ^{3,4}, defined analogously to the proton structure function F_2 .

Similarly to diffractive DIS, $ep \rightarrow eXY$, where the presence of the large scale Q allows for the application of perturbative QCD and X comprises the sum over all possible final states, many other processes with a hard scale provided by specific final states in the central system X can be predicted using QCD perturbation theory. Such processes, usually called hard diffractive processes, are e.g. dijet production in diffractive photoproduction ($Q^2 \simeq 0$) and DIS ($Q^2 \neq 0$), where the large scale is given by the jet transverse energy E_T^{jet} and possibly Q , and diffractive open heavy-flavor production, where the large scale is given by the heavy-flavor mass and possibly E_T and/or Q , in photoproduction or DIS and many more diffractive processes induced by $p\bar{p}$ or pp collisions. The central problem in hard diffraction is the problem of QCD factorization, i.e. the question whether diffractive cross sections are factorisable into universal DPDFs and partonic cross sections, which are

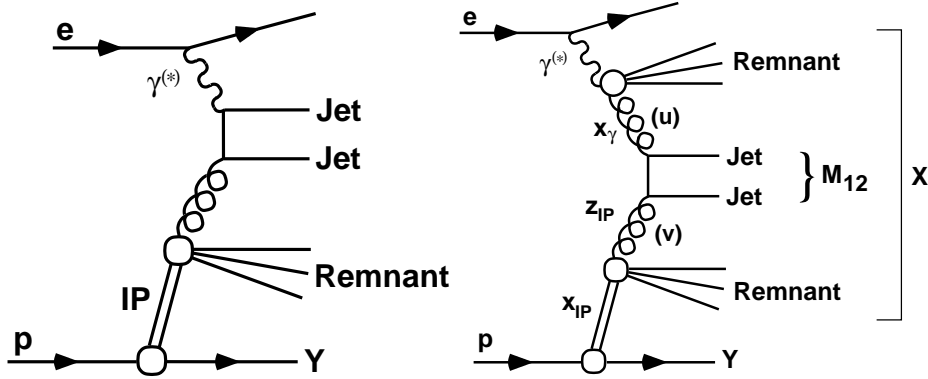


Fig. 2. Diffractive production of dijets with invariant mass M_{12} in direct (left) and resolved (right) photon-pomeron collisions, leading to the production of one or two additional remnant jets.

calculable in perturbative QCD. This question is the subject of the current debate in diffractive physics and is of particular interest for the prospects of discovery of new particles such as the Higgs boson in diffractive reactions at the LHC ^{7,8,9}.

For the inclusive DIS process, factorization has indeed been proven to hold ¹⁰, and on this basis DPDFs have been extracted at $Q^2 \neq 0$ ^{3,4,5} from high-precision inclusive measurements of the process $ep \rightarrow eXY$ using the usual DGLAP evolution equations. The proof of the factorization formula, usually referred to as the validity of QCD factorization in hard diffraction, also appears to be valid for the production of specific final states in DIS, as e.g. the production of jets or heavy-flavor particles, and for the direct part of photoproduction ($Q^2 \simeq 0$) or low- Q^2 electroproduction of jets ¹⁰. However, factorization does not hold for hard processes in diffractive hadron-hadron scattering. The problem is that soft interactions between the ingoing hadrons and/or their remnants occur in both the initial and the final state. This agrees with experimental measurements at the Tevatron ¹¹. Predictions of diffractive dijet cross sections for collisions as measured by CDF using DPDFs determined earlier by the H1 collaboration ¹² at HERA overestimate the measured cross section by up to an order of magnitude ¹¹. This large suppression of the CDF cross section can be explained by the rescattering of the two incoming hadron beams, which, by creating additional hadrons, destroy the rapidity gap ¹³.

Jet production with real photons involves direct interactions of the photon with quarks or gluons originating from the proton or pomeron, respectively, as well as resolved photon contributions leading to parton-parton interactions with an additional remnant jet coming from the photon as reviewed in ¹⁴ (see Fig. 2). For the direct interactions, we expect factorization to be valid as in the case of inclusive DIS, as already mentioned, whereas we expect it to fail for the resolved process as in hadron-hadron scattering. For this part of photoproduction we would therefore expect a similar suppression factor (sometimes also called rapidity-gap survival

probability) due to rescattering effects of the ingoing partons or hadrons. Introducing vector-meson dominance photon fluctuations, such a suppression by about a factor of three was predicted for resolved photoproduction at HERA ¹⁵.

The first measurements of dijet cross sections in diffractive photoproduction have been presented by the H1 collaboration as contributions to two conferences ¹⁶. The kinematic range for these data were $Q^2 < 0.01 \text{ GeV}^2$, $x_{\mathbb{P}} < 0.03$, $E_T^{jet1} > 5 \text{ GeV}$, $E_T^{jet2} > 4 \text{ GeV}$ and $165 < W < 240 \text{ GeV}$, where jets were identified using the inclusive k_T -cluster algorithm (the definitions of these and the following variables will be given in the next section). The measured cross sections as a function of x_γ^{obs} and $z_{\mathbb{P}}^{obs}$ were compared to leading-order (LO) QCD predictions, using the RAP-GAP Monte Carlo model ¹⁷. For the DPDFs the LO ‘H1 2002 fit’ was used ¹². The two cross sections were found to be well described by the predictions in normalization and shape over the whole range of x_γ^{obs} and $z_{\mathbb{P}}^{obs}$, showing no breakdown of factorization neither in resolved nor in direct photoproduction. In addition, normalized cross sections as a function of various other variables were compared to the predictions with the result that all measured distributions were in good agreement.

Subsequently we calculated the next-to-leading order (NLO) corrections for the cross section of diffractive dijet production using the same kinematic cuts and with the same DPDFs as in the first H1 analysis ¹⁶ on the basis of our previous work on NLO corrections for inclusive direct ¹⁸ and resolved ¹⁹ dijet photoproduction. While at LO good agreement with the H1 data ¹⁶ was found, consistent with the finding in the H1 analysis ¹⁶, it was found that the NLO corrections increase the cross section significantly ^{20,21} and require a suppression factor of the order of $R = 0.5$. Since on theoretical grounds only a suppression of the resolved cross section would be acceptable, we demonstrated in ^{20,21} that by multiplying the resolved cross section with the suppression factor $R = 0.34$, reasonably good agreement with the preliminary H1 data ¹⁶ could be achieved. This value for the suppression factor turned out to be in good agreement with the prediction of ¹⁵.

The first experimental data from the ZEUS collaboration were presented at the DIS workshop in 2004 ²². The dijet cross sections were obtained in the kinematic range $Q^2 < 1 \text{ GeV}^2$, $x_{\mathbb{P}} < 0.035$ and $E_T^{jet1(2)} > 7.5 (6.5) \text{ GeV}$. For these kinematic constraints NLO calculations were not available in 2004. So, the measurements were compared to LO calculations, unfortunately with previous H1 DPDFs ²³ with the result, that good agreement in the shape was achieved. But the normalization was off by a factor of 0.6, which was attributed to the older DPDF input ²⁴, so that the H1 and ZEUS results were consistent with each other. The situation concerning the agreement of H1 and ZEUS data and the influence of NLO corrections improved already considerably in the fall of 2004. These preliminary data from both HERA collaborations together with comparisons to NLO calculations based on the DPDF fits from ¹² were presented at workshops and conferences in the following years.

In 2006 the H1 collaboration published their final DPDF fits from their high-precision measurements using the DGLAP evolution equations ⁴. This analysis was

based on the larger data sample of the years 1997-2000 as compared to the earlier preliminary DPDF sets¹². In⁴ two DPDF sets, the 'H1 2006 fit A' and the 'H1 2006 fit B' were presented, which both give a good description of the inclusive diffractive data. These two sets differ mainly in the gluon density at large fractional parton momenta, which is poorly constrained by the inclusive diffractive scattering data, since there is no direct coupling of the photon to gluons, so that the gluon density is constrained only through the evolution. The gluon density of fit A is peaked at the starting scale at large fractional momenta, whereas fit B is flat in this region.

In 2007 the final publications for diffractive dijet production appeared²⁵. The comparison between these experimental results and the NLO theory was based on the new and final DPDFs from H1⁴. The differential cross sections as measured by H1²⁵ were compared to NLO predictions obtained with the Frixione program²⁶ interfaced to the 'H1 2006 fit B' DPDFs. The conclusions deduced earlier from the comparison with the preliminary data and the preliminary 'H1 2002 fit'¹² are fully confirmed in²⁵ with the new DPDFs fits⁴. In particular, a global suppression is obtained, independent of the DPDFs fits used, i.e. fit A or fit B, by considering the ratio of measured dijet cross sections to NLO predictions in photoproduction in relation to the same ratio in DIS. In this comparison the value of the suppression is 0.5. In addition, by using this overall suppression factor, H1 obtained a good description of all the measured distributions in the variables $z_{\mathbb{P}}^{obs}$, x_{γ}^{obs} , $x_{\mathbb{P}}$, W , E_T^{jet1} , $\bar{\eta}^{jets}$, $|\Delta\eta^{jets}|$ and M_{12} interfaced with the 'H1 2006 fit B' DPDFs and taking into account hadronization corrections²⁵. Finally, the H1 collaboration investigated how well the data are describable under the assumption that in the NLO calculation the cross section for $x_{\gamma}^{obs} > 0.9$ is not suppressed. The best agreement in a fit was obtained for a suppression factor 0.44 for the NLO calculation with $x_{\gamma}^{obs} < 0.9$, based on fitting the distributions for x_{γ}^{obs} , W , $\bar{\eta}^{jets}$ and E_T^{jet1} . In this comparison they found disagreement for the largest x_{γ}^{obs} -bin and the lowest $\bar{\eta}^{jets}$ (which are related), but better agreement in the E_T^{jet1} -distribution. In²⁵ this leads to the statement, that the assumption that the direct cross section obeys factorization is strongly disfavored by their analysis. In total, it is obvious that in the final H1 analysis²⁵ a global suppression in diffractive dijet photoproduction is clearly established and the model with resolved suppression only is not as well supported by the data.

Just recently also the ZEUS collaboration presented their final result on diffractive dijet photoproduction²⁷. As in their preliminary analysis, the two jets with the highest transverse energies E_T^{jet} were required to satisfy $E_T^{jet1(2)} > 7.5$ (6.5) GeV, which is higher than in the H1 analysis with $E_T^{jet1(2)} > 5$ (4) GeV²⁵. ZEUS compared their measurements with the NLO predictions for diffractive photoproduction of dijets based on our program²¹. Three sets of DPDFs were used, the ZEUS LPS fit, determined from a NLO analysis of inclusive diffraction and diffractive charm-production data³, and the two H1 fits, H1 2006 fit A and fit B⁴. The NLO results obtained with the two H1 fits were scaled down by a factor of 0.87⁴, since the H1 measurements used to derive the DPDFs include low-mass proton

dissociative processes with $M_Y < 1.6$ GeV, which increases the photon-diffractive cross section by $1.15^{+0.15}_{-0.08}$ as compared to the pure proton final state as corrected to in the ZEUS analysis. The comparison of the measured cross sections and the theoretical predictions was based on the distributions in the variables y , M_X , $x_{\mathcal{P}}$, $z_{\mathcal{P}}^{obs}$, E_T^{jet1} , η_{lab}^{jet1} and x_γ^{obs} . The data were reasonably well described in their shape as a function of these variables and lay systematically below the predictions. The predictions for the three DPDFs differed appreciably. The cross sections for the H1 2006 fit A (fit B) were the highest (lowest) and the one for the ZEUS LPS fit lay between the two, but nearer to the fit A than the fit B predictions. For $d\sigma/dx_\gamma^{obs}$ ZEUS also showed the ratio of the data and the NLO predictions using the ZEUS LPS fit. It was consistent with a suppression factor of 0.7 independent of x_γ^{obs} . This suppression factor depended on the DPDFs and ranged between 0.6 (H1 2006 fit A) and 0.9 (fit B). Taking into account the scale dependence of the theoretical predictions the ratio was outside the theoretical uncertainty for the ZEUS LPS fit and the H1 2006 fit A, but not for fit B. In their conclusions the authors of the ZEUS analysis²⁷ made the statement that the NLO calculations tend to overestimate the measured cross section, which would mean that a suppression is present. Unfortunately, however, they continued, that, within the large uncertainties of the NLO calculations, the data were compatible with the QCD calculations, i.e. with no suppression.

Such a statement clearly contradicts the result of the H1 collaboration²⁵ and casts doubts on the correctness of the H1 analysis. The authors of²⁷ attribute this discrepancy to the fact that the H1 measurements²⁵ were carried out in a lower E_T^{jet} and a higher $x_{\mathcal{P}}$ range than those in the ZEUS study²⁷. Besides the different E_T^{jet} and $x_{\mathcal{P}}$ regions in²⁵ and²⁷, the two measurements suffer also from different experimental cuts of some other variables, which makes it difficult to compare the two data sets directly (note also the lower center-of-mass energy for the H1 data). In addition the comparison with NLO theory in²⁵ and²⁷ was done with two different programs¹⁹ versus²⁶, which, however agreed quite well with each other²⁵.

The rather different conclusions concerning factorization breaking in diffractive dijet photoproduction calls for a new comparative study of the two data sets in²⁵ and²⁷. We have therefore performed a new calculation of the NLO cross sections on the basis of our earlier work²¹ with the new H1 2006 DPDFs and revised hadronic corrections as compared to²⁰, in order to see whether we can confirm the very different conclusions achieved in the H1²⁵ and ZEUS²⁷ analyses. In the comparison with the new data sets we shall follow more or less the same strategy as in our earlier work^{20,21}. We first calculate the unsuppressed NLO cross sections including an error band based on the scale variation and see how much and in which distribution the data points lie inside or outside this error band. Then we determine a global suppression factor by fitting the differential cross section $d\sigma/dE_T^{jet1}$ at the bin with the lowest E_T^{jet1} . With this suppression factor we shall compare to the differential cross sections of all the other measured variables and look for consistency.

In this new comparison between the experimental and the theoretical results we shall concentrate on using the H1 2006 fit B⁴ input, since it leads to smaller cross sections than the DPDFs from H1 2006 fit A⁴ or the ZEUS LPS DPDF fit³.

Actually the H1 collaboration constructed a third set of DPDFs, which is called the 'H1 2007 fit jets'. This fit is obtained through a simultaneous fit to the diffractive inclusive and DIS dijet cross sections²⁸. It is performed under the assumption that there is no factorization breaking in the diffractive dijet cross sections. Under this assumption, including the diffractive dijet cross sections in the analysis leads to additional constraints, mostly on the diffractive gluon distribution. On average the 'H1 2007 fit jets' is similar to the 'H1 2006 fit B' except for the gluon distribution at high momentum fraction and smaller factorization scales. In our analysis we shall disregard this new set of DPDFs, since it would be compatible with the factorization test of the photoproduction data only if we restricted these tests to the case that only the resolved part has this breaking and not the direct part, which has the same structure as the DIS dijet cross section.

In Sec. 2 we shall present the complete list of cuts on the experimental variables, give all the input used in the cross section calculations, and present the basic formulæ, from which the dijet cross sections have been calculated. The comparison with the H1²⁵ and the ZEUS²⁷ experimental data is presented and discussed in Sec. 3. In this comparison we shall concentrate on the main question, whether there is a suppression in the photoproduction data at all. In addition we shall investigate also whether a reasonable description of the data is possible with suppression of the resolved cross section only, as we studied it already in our previous work in 2004^{20,21}. In Sec. 4 we shall finish with a summary and our conclusions.

2. Kinematic variables and cross section formulæ

2.1. Kinematic variables and constraints

The diffractive process $ep \rightarrow eXY$, in which the systems X and Y are separated by the largest rapidity gap in the final state, is sketched in Fig. 2. The system X contains at least two jets, and the system Y is supposed to be a proton or another low-mass baryonic system. Let k and P denote the momenta of the incoming electron (or positron) and proton, respectively, and q the momentum of the virtual photon γ^* . Then the usual kinematic variables are

$$s = (k + P)^2, \quad Q^2 = -q^2, \quad \text{and} \quad y = \frac{qP}{kP}. \quad (1)$$

We denote the four-momenta of the systems X and Y by p_X and p_Y . The H1 data²⁵ are described in terms of

$$\begin{aligned} M_X^2 &= p_X^2 \quad \text{and} \quad t = (P - p_Y)^2, \\ M_Y^2 &= p_Y^2 \quad \text{and} \quad x_P = \frac{q(P - p_Y)}{qP}, \end{aligned} \quad (2)$$

Table 1. Kinematic cuts applied in the H1 analysis of diffractive dijet photoproduction.

165 GeV	<	W	<	242 GeV
		Q^2	<	0.01 GeV ²
		E_T^{jet1}	>	5 GeV
		E_T^{jet2}	>	4 GeV
-1	<	$\eta_{lab}^{jet1,2}$	<	2
		$x_{\mathcal{P}}$	<	0.03
		M_Y	<	1.6 GeV
		$-t$	<	1 GeV ²

where M_X and M_Y are the invariant masses of the systems X and Y , t is the squared four-momentum transfer of the incoming proton and the system Y , and $x_{\mathcal{P}}$ is the momentum fraction of the proton beam transferred to the system X .

The exchange between the systems X and Y is supposed to be the pomeron \mathcal{P} or any other Regge pole, which couples to the proton and the system Y with four-momentum $P - p_Y$. In this work we will neglect Reggeon exchanges, which contribute only at large $x_{\mathcal{P}}$. The pomeron is resolved into partons (quarks or gluons) with four-momentum v . In the same way the virtual photon can resolve into partons with four-momentum u , which is equal to q for the direct process. With these two momenta u and v we define

$$x_\gamma = \frac{Pu}{Pq} \text{ and } z_{\mathcal{P}} = \frac{qv}{q(P - p_Y)}. \quad (3)$$

x_γ is the longitudinal-momentum fraction carried by the partons coming from the photon, and $z_{\mathcal{P}}$ is the corresponding quantity carried by the partons of the pomeron etc., i.e. the diffractive exchange. For the direct process we have $x_\gamma = 1$. The final state, produced by the ingoing momenta u and v , has the invariant mass $M_{12} = \sqrt{(u + v)^2}$, which is equal to the invariant dijet mass in the case that no more than two hard jets are produced. $q - u$ and $P - p_Y - v$ are the four-momenta of the remnant jets produced at the photon and pomeron side. The regions of the kinematic variables, in which the cross section has been measured by the H1 collaboration²⁵, are given in Tab. 1, whereas the corresponding regions for the ZEUS analysis²⁷ are given in Tab. 2. In each case, we have evaluated the theoretical cross sections with the corresponding constraints.

The upper limit of $x_{\mathcal{P}}$ is kept small in order for the pomeron exchange to be dominant. In the experimental analysis as well as in the NLO calculations, jets are defined with the inclusive k_T -cluster algorithm with a distance parameter $d = 1$ ²⁹ in the laboratory frame. At least two jets are required with transverse energies $E_T^{jet1} > 5$ (7.5) GeV and $E_T^{jet2} > 4$ (6.5) GeV. They are the leading and subleading jets with $-1 < \eta_{lab}^{jet1,2} < 2$ ($-1.5 < \eta_{lab}^{jet1,2} < 1.5$) for H1 (ZEUS). The lower limits of the jet E_T 's are asymmetric in order to avoid infrared sensitivity in the computation of the NLO cross sections, which are integrated over E_T ³⁰.

In the experimental analysis the variable y is deduced from the energy E'_e of the

Table 2. Kinematic cuts applied in the ZEUS analysis of diffractive dijet photoproduction.

0.2	<	y	<	0.85
		Q^2	<	1 GeV ²
		E_T^{jet1}	>	7.5 GeV
		E_T^{jet2}	>	6.5 GeV
-1.5	<	$\eta_{lab}^{jet1,2}$	<	1.5
		$x_{\mathcal{P}}$	<	0.025
		$-t$	<	5 GeV ²

scattered electron, $y = 1 - E'_e/E_e$. Furthermore, $sy = W^2 = (q + P)^2 = (p_X + p_Y)^2$. The range of W given in Tab. 1 corresponds to the y range $0.3 < y < 0.65$. $x_{\mathcal{P}}$ is reconstructed according to

$$x_{\mathcal{P}} = \frac{\sum_X (E + p_z)}{2E_p}, \quad (4)$$

where E_p is the proton beam energy and the sum runs over all particles (jets) in the X -system. The variables M_{12} , x_γ , and $z_{\mathcal{P}}$ are determined only from the kinematic variables of the two hard leading jets with four-momenta p^{jet1} and p^{jet2} . So,

$$M_{12}^2 = (p^{jet1} + p^{jet2})^2, \quad (5)$$

where additional jets are not taken into account. In the same way we have

$$x_\gamma^{\text{obs}} = \frac{\sum_{\text{jets}} (E - p_z)}{2yE_e} \quad \text{and} \quad z_{\mathcal{P}}^{\text{obs}} = \frac{\sum_{\text{jets}} (E + p_z)}{2x_{\mathcal{P}}E_p}. \quad (6)$$

The sum over jets runs only over the variables of the two leading jets. These definitions for x_γ and $z_{\mathcal{P}}$ are not the same as the definitions given earlier, where also the remnant jets and any additional hard jets are taken into account in the final state. In the same way M_X can be estimated by $M_X^2 = M_{12}^2 / (z_{\mathcal{P}}^{\text{obs}} x_\gamma^{\text{obs}})$. The dijet system is characterized by the transverse energies E_T^{jet1} and E_T^{jet2} and the rapidities in the laboratory system η_{lab}^{jet1} and η_{lab}^{jet2} . The differential cross sections are measured and calculated as functions of the transverse energy E_T^{jet1} of the leading jet, the average rapidity $\bar{\eta}^{jets} = (\eta_{lab}^{jet1} + \eta_{lab}^{jet2})/2$, and the jet separation $|\Delta\eta^{jets}| = |\eta_{lab}^{jet1} - \eta_{lab}^{jet2}|$, which is related to the scattering angle in the center-of-mass system of the two jets.

2.2. Diffractive parton distributions

The diffractive PDFs are obtained from an analysis of the diffractive process $ep \rightarrow eXY$, which is illustrated in Fig. 1, where now Q^2 is large and the state X consists of all possible final states, which are summed. The cross section for this diffractive DIS process depends in general on five independent variables (azimuthal angle dependence neglected): Q^2 , x (or β), $x_{\mathcal{P}}$, M_Y , and t . These variables are defined as before, and $x = Q^2/(2Pq) = Q^2/(Q^2 + W^2) = x_{\mathcal{P}}\beta$. The system Y is not measured, and the results are integrated over $-t < 1 \text{ GeV}^2$ and $M_Y < 1.6 \text{ GeV}$

10 *M. Klasen, G. Kramer*

as in the photoproduction case. The measured cross section is expressed in terms of a reduced diffractive cross section $\sigma_r^{D(3)}$ defined through

$$\frac{d^3\sigma^D}{dx_{\mathbb{P}}dx dQ^2} = \frac{4\pi\alpha^2}{xQ^4} \left(1 - y + \frac{y^2}{2}\right) \sigma_r^{D(3)}(x_{\mathbb{P}}, x, Q^2) \quad (7)$$

and is related to the diffractive structure functions $F_2^{D(3)}$ and $F_L^{D(3)}$ by

$$\sigma_r^{D(3)} = F_2^{D(3)} - \frac{y^2}{1 + (1 - y)^2} F_L^{D(3)}. \quad (8)$$

y is defined as before, and $F_L^{D(3)}$ is the longitudinal diffractive structure function.

The proof of Collins¹⁰, that QCD factorization is applicable to diffractive DIS, has the consequence that the DIS cross section for $\gamma^*p \rightarrow XY$ can be written as a convolution of a partonic cross section $\sigma_a^{\gamma^*}$, which is calculable as an expansion in the strong coupling constant α_s , with diffractive PDFs f_a^D yielding the probability distribution for a parton a in the proton under the constraint that the proton undergoes a scattering with a particular value for the squared momentum transfer t and $x_{\mathbb{P}}$. Then the cross section for $\gamma^*p \rightarrow XY$ is

$$\frac{d^2\sigma}{dx_{\mathbb{P}}dt} = \sum_a \int_x^{x_{\mathbb{P}}} d\xi \sigma_a^{\gamma^*}(x, Q^2, \xi) f_a^D(\xi, Q^2; x_{\mathbb{P}}, t). \quad (9)$$

This formula is valid for sufficiently large Q^2 and fixed $x_{\mathbb{P}}$ and t . The parton cross sections are the same as those for inclusive DIS. The diffractive PDFs are non-perturbative objects. Only their Q^2 -evolution can be predicted with the well-known DGLAP evolution equations², which we shall use in NLO.

Usually for $f_a^D(x, Q^2; x_{\mathbb{P}}, t)$ an additional assumption is made, namely that it can be written as a product of two factors, $f_{\mathbb{P}/p}(x_{\mathbb{P}}, t)$ and $f_{a/\mathbb{P}}(\beta, Q^2)$,

$$f_a^D(x, Q^2; x_{\mathbb{P}}, t) = f_{\mathbb{P}/p}(x_{\mathbb{P}}, t) f_{a/\mathbb{P}}(\beta = x/x_{\mathbb{P}}, Q^2). \quad (10)$$

$f_{\mathbb{P}/p}(x_{\mathbb{P}}, t)$ is the pomeron flux factor. It gives the probability that a pomeron with variables $x_{\mathbb{P}}$ and t couples to the proton. Its shape is controlled by Regge asymptotics and is in principle measurable by soft processes under the condition that they can be fully described by single-pomeron exchange. This Regge factorization formula represents the resolved pomeron model, in which the diffractive exchange, i.e. the pomeron, can be considered as a quasi-real particle with a partonic structure given by PDFs $f_{a/\mathbb{P}}(\beta, Q^2)$. β is the longitudinal momentum fraction of the pomeron carried by the emitted parton a in the pomeron. The important point is that the dependence of f_a^D on the four variables $x, Q^2, x_{\mathbb{P}}$ and t factorizes into two functions $f_{\mathbb{P}/p}$ and $f_{a/\mathbb{P}}$, which each depend only on two variables.

Since the value of t could not be fixed in the diffractive DIS measurements, it is integrated over with t in the region $t_{\text{cut}} < t < t_{\text{min}}$. Therefore we have^{4,12}

$$f(x_{\mathbb{P}}) = \int_{t_{\text{cut}}}^{t_{\text{min}}} dt f_{\mathbb{P}/p}(x_{\mathbb{P}}, t), \quad (11)$$

where $t_{\text{cut}} = -1 \text{ GeV}^2$ and t_{min} is the minimum kinematically allowed value of $|t|$. In ^{12,4} the pomeron flux factor is assumed to have the form

$$f_{\mathbb{P}/p}(x_{\mathbb{P}}, t) = x_{\mathbb{P}}^{1-2\alpha_{\mathbb{P}}(t)} \exp(B_{\mathbb{P}}t). \quad (12)$$

$\alpha_{\mathbb{P}}(t)$ is the pomeron trajectory, $\alpha_{\mathbb{P}}(t) = \alpha_{\mathbb{P}}(0) + \alpha'_{\mathbb{P}}t$, assumed to be linear in t . The values of $B_{\mathbb{P}}$, $\alpha_{\mathbb{P}}(0)$ and $\alpha'_{\mathbb{P}}$ are taken from ⁴ and have the values $B_{\mathbb{P}} = 5.5 \text{ GeV}^{-2}$, $\alpha_{\mathbb{P}}(0) = 1.118$ (fit A), $\alpha_{\mathbb{P}}(0) = 1.111$ (fit B) and $\alpha'_{\mathbb{P}} = 0.06 \text{ GeV}^{-2}$. Usually $f_{\mathbb{P}/p}(x_{\mathbb{P}}, t)$ as written in Eq. (12) has in addition to the dependence on $x_{\mathbb{P}}$ and t a normalization factor N , which can be inferred from the asymptotic behavior of σ_{tot} for pp and $p\bar{p}$ scattering. Since it is unclear whether these soft diffractive cross sections are dominated by a single pomeron exchange, it is better to include N into the pomeron PDFs $f_{a/\mathbb{P}}$ and fix it from the diffractive DIS data ⁴. The diffractive DIS cross section $\sigma_r^{D(3)}$ is measured in the kinematic range $3.5 \leq Q^2 \leq 1600 \text{ GeV}^2$, $0.01 \leq \beta \leq 0.9$ and $10^{-4} \leq x_{\mathbb{P}} < 0.05$.

The pomeron couples to quarks in terms of a light flavor singlet $\Sigma(z_{\mathbb{P}}) = u(z_{\mathbb{P}}) + d(z_{\mathbb{P}}) + s(z_{\mathbb{P}}) + \bar{u}(z_{\mathbb{P}}) + \bar{d}(z_{\mathbb{P}}) + \bar{s}(z_{\mathbb{P}})$ and to gluons in terms of $g(z_{\mathbb{P}})$, which are parameterized at the starting scale $Q_0^2 = 1.75 \text{ GeV}^2$ (fit A) and 2.5 GeV^2 (fit B). $z_{\mathbb{P}}$ is the momentum fraction entering the hard subprocess, so that for the LO process $z_{\mathbb{P}} = \beta$, and in NLO $\beta < z_{\mathbb{P}} < 1$. These PDFs of the pomeron are parameterized by a particular form in terms of the usual power ansatz as given in ⁴. Charm quarks and bottom quarks couple differently from the light quarks by including the finite charm mass $m_c = 1.4 \text{ GeV}$ and bottom mass $m_b = 4.5 \text{ GeV}$ in the massive quark scheme and describing the coupling to photons via the photon-gluon fusion type process up to order α_s^2 . For the pomeron PDFs, we used a two-dimensional fit in the variables $z_{\mathbb{P}}$ and Q^2 and then inserted the interpolated result in the cross section formula.

2.3. Cross section formula

Under the assumption that the cross section can be calculated from the well-known formulæ for jet production in low- Q^2 ep collisions, the cross section for the reaction $e + p \rightarrow e + 2 \text{ jets} + X' + Y$ is computed from the following basic formula:

$$\begin{aligned} d\sigma^D(ep \rightarrow e + 2 \text{ jets} + X' + Y) = & \\ \sum_{a,b} \int_{t_{\text{cut}}}^{t_{\text{min}}} dt \int_{x_{\mathbb{P}}^{\text{min}}}^{x_{\mathbb{P}}^{\text{max}}} dx_{\mathbb{P}} \int_0^1 dz_{\mathbb{P}} \int_{y_{\text{min}}}^{y_{\text{max}}} dy \int_0^1 dx_{\gamma} & \\ f_{\gamma/e}(y) f_{a/\gamma}(x_{\gamma}, M_{\gamma}^2) f_{\mathbb{P}/p}(x_{\mathbb{P}}, t) f_{b/\mathbb{P}}(z_{\mathbb{P}}, M_{\mathbb{P}}^2) & \\ d\sigma^{(n)}(ab \rightarrow \text{jets}). & \end{aligned} \quad (13)$$

y , x_{γ} and $z_{\mathbb{P}}$ denote the longitudinal momentum fractions of the photon in the electron, the parton a in the photon, and the parton b in the pomeron. M_{γ} and $M_{\mathbb{P}}$ are the factorization scales at the respective vertices, and $d\sigma^{(n)}(ab \rightarrow \text{jets})$ is the

12 *M. Klasen, G. Kramer*

cross section for the production of an n -parton final state from two initial partons a and b . It is calculated in NLO, as are the PDFs of the photon and the pomeron.

The function $f_{\gamma/e}(y)$, which describes the virtual photon spectrum, is assumed to be given by the well-known Weizsäcker–Williams approximation,

$$f_{\gamma/e}(y) = \frac{\alpha}{2\pi} \left[\frac{1 + (1-y)^2}{y} \ln \frac{Q_{\max}^2(1-y)}{m_e^2 y^2} + 2m_e^2 y \left(\frac{1-y}{m_e^2 y^2} - \frac{1}{Q_{\max}^2} \right) \right]. \quad (14)$$

Usually, only the dominant leading logarithmic contribution is considered. We have added the second non-logarithmic term as evaluated in ³¹. $Q_{\max}^2 = 0.01$ (1) GeV^2 for the H1 (ZEUS) cross sections calculated in this work.

The formula for the cross section $d\sigma^D$ can be used for the resolved as well as for the direct process. For the latter, the parton a is the photon and $f_{\gamma/\gamma}(x_\gamma, M_\gamma^2) = \delta(1-x_\gamma)$, which does not depend on M_γ . As is well known, the distinction between direct and resolved photon processes is meaningful only in LO of perturbation theory. In NLO, collinear singularities arise from the photon initial state, that must be absorbed into the photon PDFs and produce a factorization scheme dependence as in the proton and pomeron cases. The separation between the direct and resolved processes is an artifact of finite order perturbation theory and depends in NLO on the factorization scheme and scale M_γ . The sum of both parts is the only physically relevant quantity, which is approximately independent of the factorization scale M_γ due to the compensation of the scale dependence between the NLO direct and the LO resolved contribution. For the resolved process, PDFs of the photon are needed, for which we choose the NLO versions of GRV ³² transformed to the $\overline{\text{MS}}$ scheme.

3. Results

3.1. Comparison with H1 data

In this section, we present the comparison of the various theoretical predictions in NLO with the experimental data from the H1 collaboration ²⁵. The corresponding kinematic cuts are given in Tab. 1. Before we confront the calculated cross sections with the experimental data, we correct them for hadronization effects. The hadronization corrections are calculated by means of the LO RAPGAP Monte Carlo generator ¹⁷. The factors for the transformation from jets made up of stable hadrons to parton jets were supplied by the H1 collaboration ²⁵. Most of our calculations are done with the ‘H1 2006 fit B’ ⁴ DPDFs since they give they smaller diffractive dijet cross sections as compared to the ‘H1 2006 fit A’. These DPDF fits are based on $n_f = 3$ massless flavors. The production of charm and bottom quarks was treated there in the Fixed-Flavor Number Scheme (FFNS) in NLO with non-zero charm and bottom quark mass. Instead of this extra treatment of the charm and bottom contribution in the pomeron we added a charm PDF in the pomeron as obtained in the ‘H1 2002 fit’ ¹², where the charm quark was also considered to be massless.

The bottom contribution was neglected. This assumption simplifies the calculations considerably. Since the charm contribution from the pomeron is small, this should be a good approximation. We then take $n_f = 4$ with $\Lambda_{\overline{\text{MS}}}^{(4)} = 0.347$ GeV, which corresponds to the value used in the DPDFs ‘H1 2006 fit A’ and ‘H1 2006 fit B’⁴.

As it is clear from the discussion of the various preliminary analyses of the H1 and ZEUS collaborations, there are two questions which we would like to answer from the comparison with the recent H1 and the ZEUS data. The first question is whether a suppression, which differs substantially from one, is needed to describe the data. The second question is whether the data are also consistent with a suppression factor applied to the resolved cross section only. To give an answer to these two questions we calculated first the cross sections with no suppression factor ($R = 1$ in the following figures) with a theoretical error obtained from varying the common scale of renormalization and factorization by factors of 0.5 and 2 around the central scale (highest E_T^{jet}). In a second step we show the results for the same differential cross sections with a global suppression factor, adjusted to $d\sigma/dE_T^{jet1}$ in the smallest E_T^{jet1} -bin. As in the experimental analysis²⁵, we consider the differential cross sections in the variables x_γ^{obs} , $z_{\mathcal{P}}^{obs}$, $\log_{10}(x_{\mathcal{P}})$, E_T^{jet1} , M_{12} , $\bar{\eta}^{jets}$, $|\Delta\eta^{jets}|$ and W .

The unsuppressed ($R = 1$) cross sections $d\sigma/dx_\gamma^{obs}$, $d\sigma/dz_{\mathcal{P}}^{obs}$, $d\sigma/d\log_{10}(x_{\mathcal{P}})$, $d\sigma/dE_T^{jet1}$, $d\sigma/dM_{12}$, $d\sigma/d\bar{\eta}^{jets}$, $d\sigma/d|\Delta\eta^{jets}|$ and $d\sigma/dW$ ($\bar{\eta}^{jets} \equiv \langle \eta_{lab}^{jet} \rangle$ in²⁵) with their scale variation are shown in Fig. 3a-h. In these figures we also plotted the experimental data with their errors. Except for two points (largest $z_{\mathcal{P}}^{obs}$ and largest E_T^{jet1} -bin) all other experimental points lie, including their errors, outside the theoretical error band. This comparison clearly tell us, that an unsuppressed cross section is in disagreement with the data. It is clear, that with the DPDFs ‘H1 2006 fit A’ cross section this conclusion would be even stronger, since with these DPDFs the unsuppressed cross sections are even larger. That $d\sigma/dz_{\mathcal{P}}^{obs}$ overlaps in the largest bin with the lower limit of the prediction for $R = 1$ (see Fig. 3b) can be explained with the fact that the gluon DPDF in the ‘H1 2006 fit B’ is not very well constrained for large β and might be larger there.

If we now determine the suppression factor from fitting the lowest E_T^{jet1} -bin experimental cross section we obtain $R = 0.42 \pm 0.06$. The indicated error corresponds to the experimental uncertainty, while we show in the figures explicitly the theoretical uncertainty. With this suppression factor we have calculated the eight distributions including their theoretical errors and compare with the experimental data including their errors. The results of this comparison is shown also in Figs. 3a-h. With the exception of Figs. 3d and 3h, where the comparisons of $d\sigma/dE_T^{jet1}$ and $d\sigma/dM_{12}$ are shown, all other plots are such that the data points lie inside the error band based on the scale variation. Most of the data points even agree with the $R = 0.42$ predictions inside the much smaller experimental errors. In $d\sigma/dE_T^{jet1}$ (see Fig. 3d) the predictions for the second and third bin lie outside the data points with their errors. For $R = 1$ and $R = 0.42$ these cross sections falls off stronger with increasing E_T^{jet1} than the data, the normalization being of course about two

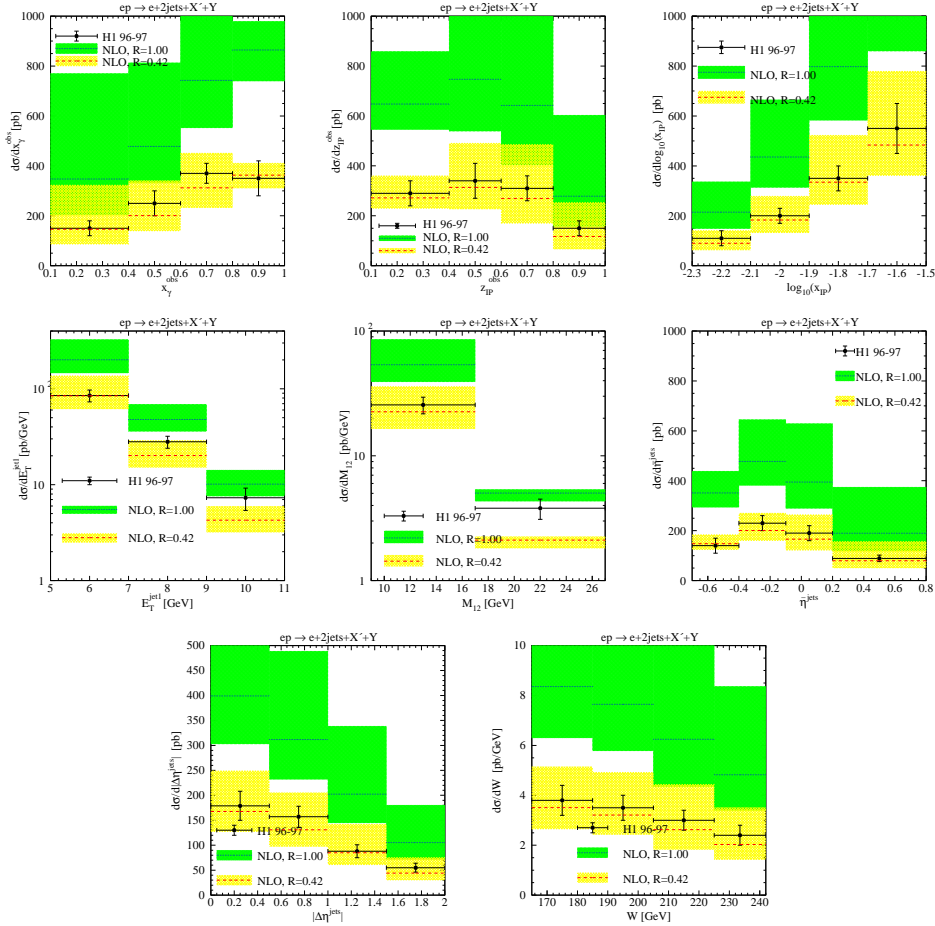
14 *M. Klasen, G. Kramer*


Fig. 3. Differential cross sections for diffractive dijet photoproduction as measured by H1 and compared to NLO QCD without ($R = 1$) and with ($R = 0.42$) global suppression (color online).

times larger for $R = 1$. In particular, the third data point agrees with the $R = 1$ prediction. This means that the suppression decreases with increasing E_T^{jet1} . Such a behavior points in the direction that a suppression of the resolved cross section only would give better agreement with the data, as we shall see below. The same observations can be made by looking at $d\sigma/dM_{12}$ in Fig. 3e. The survival probability $R = 0.42 \pm 0.06$ agrees with the result in ²⁵, which quotes $R = 0.50 \pm 0.10$, determined by a fit to the double ratio of measured to predicted cross section in photoproduction by the corresponding ratio in DIS given as a function of W . In this double ratio many experimental errors and theoretical scale errors cancel to a large extent. This double ratio is also insensitive to the detailed shape of the diffractive gluon density. From our comparison we conclude that the H1 data show a global suppression of the order of two in complete agreement with the results ^{20,21} and

²⁵ based on earlier preliminary ¹⁶ and final H1 data ²⁵.

Next we want to answer the second question, whether the data could be consistent with a suppression of the resolved component only. For this purpose we have calculated the cross sections in two versions: (i) suppression of the resolved cross section and (ii) suppression of the resolved cross section plus that part of the NLO direct part which depends on the factorization scale at the photon vertex and thereby eliminates the M_γ -dependence in the combined direct and resolved cross section ³³. Of course, the needed suppression factors for the two versions will be different. We determine the suppression factors by fitting again the measured $d\sigma/dE_T^{jet1}$ for the lowest E_T^{jet1} -bin (see Fig. 4d). Then, the suppression factor for version (i) is $R = 0.31$ (denoted res in the figures), and for version (ii) it is $R = 0.29$ (denoted res+dir-IS). The comparison with the H1 data of $d\sigma/dx_\gamma^{obs}$, $d\sigma/dz_P^{obs}$, $d\sigma/d\log_{10}(x_P)$, $d\sigma/dE_T^{jet1}$, $d\sigma/dM_{12}$, $d\sigma/d\bar{\eta}^{jets}$, $d\sigma/d|\Delta\eta^{jets}|$ and $d\sigma/dW$ is shown in Figs. 4a-h, where we also have plotted the prediction for the global suppression (direct and resolved) with $R = 0.42$, already shown in Figs. 3a-h. Looking at Figs. 4a-h we can distinguish three groups of results from the comparison with the data. In the first group, the cross sections as functions of z_P^{obs} , $\log_{10}(x_P)$, M_{12} , $|\Delta\eta^{jets}|$ and W , the agreement with the global suppression ($R = 0.42$) and the resolved suppression ($R = 0.31$ and $R = 0.29$) is comparable. In the second group, which consists just of $d\sigma/dE_T^{jet1}$, the agreement is better for the resolved suppression only. In the third group, $d\sigma/dx_\gamma^{obs}$ and $d\sigma/d\bar{\eta}^{jets}$, the agreement with the resolved suppression is worse than with the global suppression. In particular, for $d\sigma/dx_\gamma^{obs}$, which is usually considered as the characteristic distribution for distinguishing global versus resolved suppression, the agreement with resolved suppression does not improve. Unfortunately, this cross section has the largest hadronic corrections of the order of $(25 - 30)\%$ ²⁵. Here, the bins with largest x_γ^{obs} are particularly sensitive to the hadronic corrections and possible migrations of the data between the two bins. If we average the cross sections for these two bins, the agreement with the data point becomes much better. We also notice, that the predictions for the two suppression modes (i) and (ii) are almost the same. The only exception are the cross sections for the largest x_γ^{obs} -bin (see Fig. 4a). In Figs. 4a-h the theoretical errors coming from the scale uncertainty are not shown. If they are taken into account, the difference between experimental data and theory in Figs. 4a and 4f is much less dramatic. On the other hand, for the cross section $d\sigma/dE_T^{jet1}$ the agreement improves considerably with the suppression of the resolved part only (note the logarithmic scale in Fig. 4d). Here, of course, we must admit that the suppression factor could be E_T -dependent, although we do not know of any mechanism, which could cause such a E_T^{jet} -dependence of the suppression. We remark that this E_T^{jet} -dependence of the global suppression is also visible in the H1 analysis of ²⁵.

We also checked for two distributions whether the predictions for resolved suppression depend on the chosen diffractive PDFs. For this purpose we have calculated for the two cases $d\sigma/dz_P^{obs}$ and $d\sigma/dE_T^{jet1}$ the cross sections with the ‘H1 2006 fit

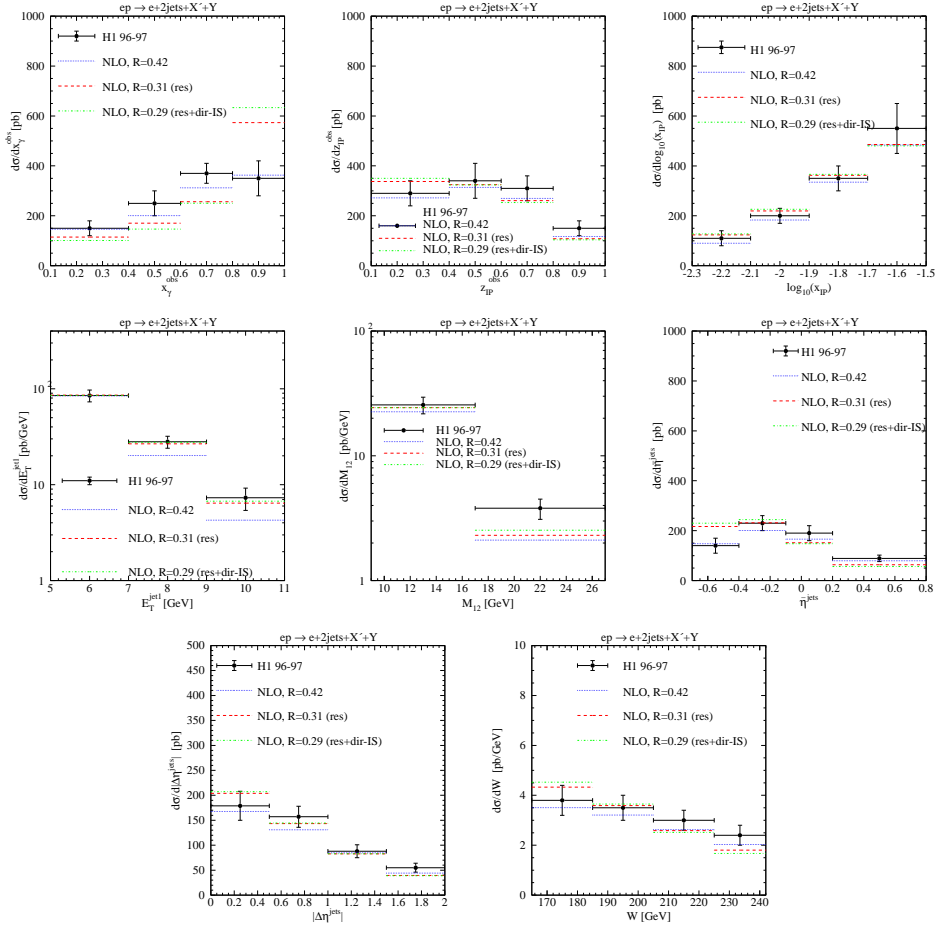
16 *M. Klasen, G. Kramer*


Fig. 4. Differential cross sections for diffractive dijet photoproduction as measured by H1 and compared to NLO QCD with global, resolved, and resolved/direct-ISR suppression.

A' parton distributions⁴. The results are compared in Figs. 5a and b to the results with the 'H1 2006 fit B' and the experimental data. Of course, since the 'H1 2006 fit A' PDFs have a larger gluon component at large β , the cross sections are larger and therefore need a larger suppression factor $R = 0.22$. From Figs. 5a and b we conclude that there is no appreciable dependence on the chosen DPDFs. Note that in Fig. 5b the cross section for the smallest E_T^{jet1} -bin has been fitted to determine the suppression factor. In total, we are tempted to conclude from the comparisons in Figs. 4a-h that the predictions with a resolved-only (or resolved+direct-ISR) suppression are consistent with the H1 data²⁵. The only exceptions are two bins in the x_γ^{obs} and one bin in the $\bar{\eta}^{jets}$ -distribution.

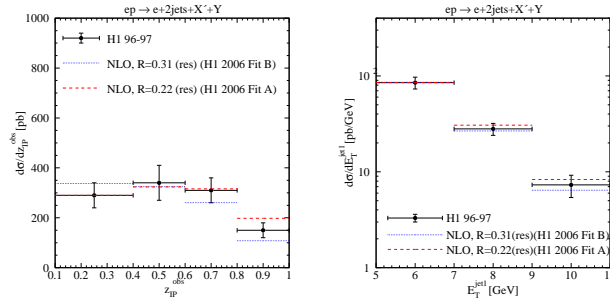


Fig. 5. Differential cross sections for diffractive dijet photoproduction as measured by H1 and compared to NLO QCD with resolved suppression and two different DPDFs.

3.2. Comparison with ZEUS data

In this subsection we shall compare our predictions with the final analysis of the ZEUS data, which was published just recently²⁷. The kinematic cuts are given in Tab. 2. There are the following differences to the H1 cuts in Tab. 1: First the upper cut on Q^2 is larger. Second there is a larger range in the variable y and the upper cut on x_P is slightly smaller. The most important change is the larger $E_T^{jet1(2)}$ cut, namely $E_T^{jet1(2)} > 7.5$ (6.5) GeV, which leads to smaller cross sections. Also the cut on $|t|$ is different. The different cuts on Q^2 and $|t|$ have little influence. For example, the larger $|t|$ -cut in Tab. 2 as compared to Tab. 1 increases the cross section only by 0.2%. The constraint on M_Y is not explicitly given in the ZEUS publication²⁷. They give the cross section for the case that the diffractive final Y state consists only of the proton. For this they correct their measured cross section by subtracting in all bins the estimated contribution of a proton-dissociative background of 16%. When comparing to the theoretical predictions with the DPDFs from the H1 2006 fits, they multiply the theoretical cross section with a (slightly different) factor of 0.87 in order to correct for the proton-dissociative contributions, which are contained in these DPDFs by requiring $M_Y < 1.6$ GeV. We do not follow this procedure. Instead we leave the theoretical cross sections unchanged, i.e. they contain a proton-dissociative contribution with $M_Y < 1.6$ GeV and multiply the ZEUS cross sections by 1.15 to include the proton-dissociative contribution. In this comparison we shall follow the same strategy as before. Before we do this, we correct our theoretical prediction by the hadronization corrections reported in²⁷. We first compare to the predictions with no suppression ($R = 1$) and then determine a suppression factor by fitting $d\sigma/dE_T^{jet1}$ at the smallest E_T^{jet1} -bin. Then we compare to the cross sections as a function of the seven observables x_γ^{obs} , z_P^{obs} , x_P , E_T^{jet1} , y , M_X and η^{jet1} instead of the eight variables in the H1 analysis. The distribution in y is equivalent to the W -distribution in²⁵. The ZEUS collaboration have also published experimental measurements in the two regions $x_\gamma < (\geq) 0.75$, which do however not consider here due to space limitations.

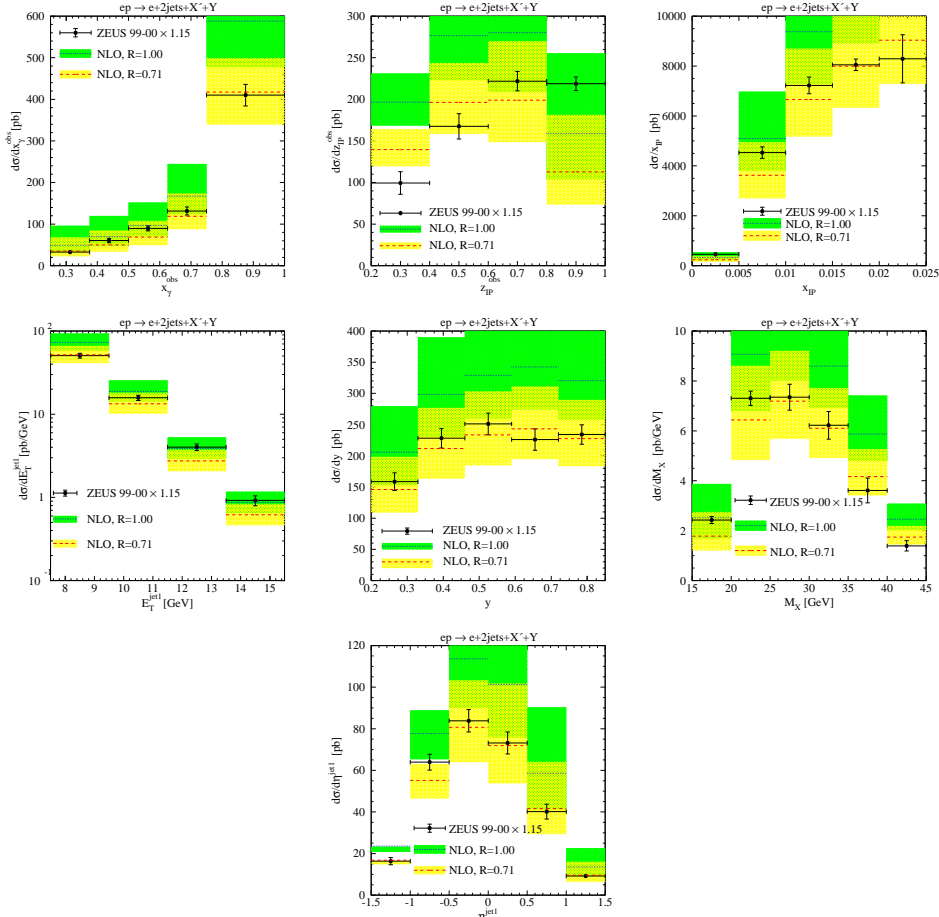
18 *M. Klasen, G. Kramer*


Fig. 6. Differential cross sections for diffractive dijet photoproduction as measured by ZEUS and compared to NLO QCD without ($R = 1$) and with ($R = 0.71$) global suppression (color online).

The theoretical predictions for these differential cross sections with no suppression factor ($R = 1$) are shown in Figs. 6a-g, together with their scale errors and compared to the ZEUS data points. Except for the x_γ^{obs} and E_T^{jet1} distributions, most of the data points lie outside the theoretical error bands for $R = 1$. In particular, in Figs. 6b, c, e, f and g, 2, 3, 4, 4 and 5 points lie outside. This means that most of the data points disagree with the unsuppressed prediction. Next, we determine the suppression factor from the measured $d\sigma/dE_T^{jet1}$ at the lowest E_T^{jet1} -bin, $7.5 \text{ GeV} < E_T^{jet1} < 9.5 \text{ GeV}$, and obtain $R = 0.71 \pm 0.06$. The indicated error corresponds again to the experimental uncertainty, while we show in the figures explicitly the theoretical uncertainty. This means that the suppression factor from the ZEUS data is larger than the one obtained from the analysis of the H1 data, which is actually consistent with the $d\sigma/dE_T^{jet1}$ for the second bin in Fig. 3b. Here

the cross section is approximately larger by a factor of 1.8 than the prediction with $R = 0.41$. If we now check how the predictions for $R = 0.71$ compare to the data points inside the theoretical errors, we observe from Figs. 6a-g that with the exception of $d\sigma/dz_{\mathbb{P}}^{obs}$ (largest bin), the data points agree with the predictions inside the theoretical error band. This is quite consistent with the H1 analysis, discussed in the previous subsection, and leads to the conclusion that also the ZEUS data agree much better with the suppressed predictions than with the unsuppressed one. In particular, the global suppression factor approximately agrees with the global suppression factor, which one would expect from the analysis of the H1 data at the second smallest E_T^{jet1} -bin.

Similarly as in the previous section we compared the ZEUS data also with the assumption that the suppression results only from the resolved cross section. Here we consider again the two versions: (i) only resolved suppression (res) and (ii) resolved plus direct suppression of the initial-state singular part (res+dir-IS). For these two models we obtain the suppression factors $R = 0.53$ and $R = 0.45$, respectively, where these suppression factors are again obtained by fitting the data point at the first bin of $d\sigma/dE_T^{jet1}$. The comparison to the global suppression with $R = 0.71$ and to the data is shown in Figs. 7a-g. In general, we observe that the difference between global suppression and resolved suppression is not large, i.e. the data points agree with the resolved suppression almost as well as with the global suppression.

In Figs. 8a and b the difference between ‘H1 2006 fit B’ and ‘H1 2006 fit A’ is shown again for the case of the resolved suppression. In both figures we observe that the fit A suppression with the suppression factor $R = 0.27$ agrees better with the data than with the factor $R = 0.53$ for the fit B suppression. In particular, for $d\sigma/dE_T^{jet1}$ the agreement with the three data points is perfect (note the logarithmic scale).

4. Conclusion

In summary, we have revisited the final H1 and ZEUS data on the diffractive photoproduction of dijets at HERA. We focused on the question if the two data sets, taken with different ep center-of-mass energies and kinematic cuts (in particular on the jet transverse energies), could be consistently interpreted within QCD factorization, employing universal parton densities in the diffractive exchange and process-specific hard partonic cross sections evaluated at NLO, or showed rather evidence of factorization breaking in the direct and/or resolved photon channels.

First, we found that even with the most optimistic (and likely realistic) parton density set ‘H1 2006 fit B’, both the H1 and ZEUS data sets were overestimated by the unsuppressed NLO predictions and better described by global suppression factors of 0.42 ± 0.06 and 0.71 ± 0.06 , respectively. These factors were obtained by fitting our NLO predictions in both cases to the lowest (and dominant) E_T^{jet} -bin and are in agreement with the global suppression factor of 0.50 ± 0.10 found by the H1 collaboration in a fit to all of their data points, but at variance with the final

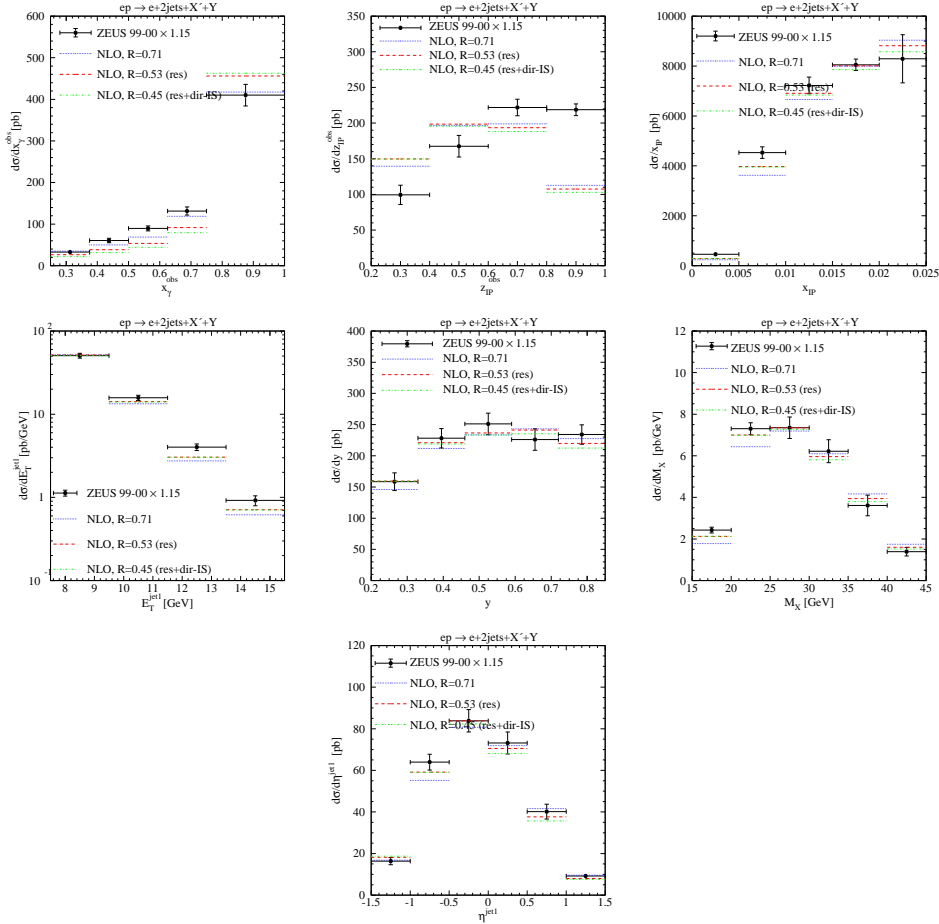
20 *M. Klasen, G. Kramer*


Fig. 7. Differential cross sections for diffractive dijet photoproduction as measured by ZEUS and compared to NLO QCD with global, resolved, and resolved/direct-IS suppression.

conclusion in the publication by the ZEUS collaboration.

Second, we demonstrated that the H1 (ZEUS) data (in particular the E_T -distributions and somewhat less the x_γ -distributions, which are unfortunately subject to large hadronization uncertainties) can be described almost equally well by applying a suppression factor of about one-third (one-half) to the resolved-only contribution. We showed that this could be consistently done by suppressing also the direct initial-state singular part without a big impact on the suppression factor with the added advantage of preserved factorization-scale invariance. Alternatively, we admitted for the possibility that a global suppression factor might be E_T^{jet} -dependent, although a theoretical motivation is only known for the first scenario and the suppression factor obtained is in good agreement with absorptive-model predictions.

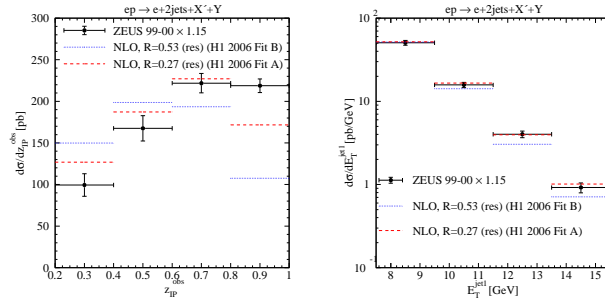


Fig. 8. Differential cross sections for diffractive dijet photoproduction as measured by ZEUS and compared to NLO QCD with resolved suppression and two different DPDFs.

Finally, we showed that our conclusions, while the numerical values of the suppression factors may change to some extent, are not qualitatively altered, when a different set of diffractive parton densities (e.g. ‘H1 2006 fit A’) is employed. The same observation should hold for the very recent ‘H1 2007 fit jets’, which is very similar to the ‘H1 2006 fit B’.

While the epoch of HERA experiments has now ended and an International Linear Collider may not be built in the near future, it will be very interesting to investigate diffractive physics at the LHC. As stated above, the search for Higgs bosons may benefit in an important way from the diffractive production channels, and this depends crucially on an excellent understanding of the QCD backgrounds. Proton-proton and heavy-ion collisions at the LHC may even be a source of high-energy photon collisions, and this may open up a whole new field of investigation for diffractive dijet photoproduction ³⁴.

References

1. P.D.B. Collins, *An Introduction to Regge Theory and High Energy Physics*, Cambridge University Press (1977); A.C. Irving and R.P. Worden, *Phys. Rept.* **34**, 117 (1977).
2. V.N. Gribov and L.N. Lipatov, *Sov. J. Nucl. Phys.* **5**, 438 (1972); *Sov. J. Nucl. Phys.* **20**, 94 (1975); G. Altarelli and G. Parisi, *Nucl. Phys. B* **126**, 298 (1977); Y.L. Dokshitzer, *Sov. Phys. JETP* **46**, 641 (1977).
3. ZEUS Collaboration, S. Chekanov et al., *Eur. Phys. J. C* **38**, 43 (2004).
4. H1 Collaboration, A. Atkas et al., *Eur. Phys. J. C* **48**, 715 (2006).
5. M. Groy, A. Levy and A. Proburyakov, Proc. of the Workshop on *HERA and the LHC*, H. Jung and A. de Roeck (eds.), CERN-2005-014, DESY-PROC-2005-001, p. 499 (2005), also hep-ph/0601012.
6. A.D. Martin, M.G. Ryskin and G. Watt, *Phys. Lett. B* **644**, 131 (2007).
7. V.A. Khoze, A.D. Martin and M.G. Ryskin, *Eur. Phys. J. C* **14**, 525 (2000); arXiv:0802.0177 [hep-ph] and further references therein.
8. M. Boonekamp, R. Peschanski and C. Royon, *Phys. Rev. Lett* **87**, 251806 (2001).
9. E. Levin, U. Maor, E. Naftali and A. Prygarin, hep-ph/0511060; Proc. of the Workshop on *HERA and the LHC*, H. Jung and A. de Roeck (eds.), CERN-2005-014, DESY-PROC-2005-001, p. 221 (2005) and further references therein.

22 M. Klasen, G. Kramer

10. J.C. Collins, *Phys. Rev. D* **57**, 3051 (1998); *ibid.* **61**, 019902 (2000) (E); *J. Phys. G* **28**, 1069 (2002).
11. CDF Collaboration, T. Affolder et al., *Phys. Rev. Lett.* **84**, 5043 (2000).
12. H1 Collaboration, paper 980, submitted to the 31st *Int. Conf. on High Energy Physics* (ICHEP), Amsterdam (2002).
13. A.B. Kaidalov, V.A. Khoze, A.D. Martin and M.G. Ryskin, *Eur. Phys. J. C* **21**, 521 (2001).
14. M. Klasen, *Rev. Mod. Phys.* **74**, 1221 (2002).
15. A.B. Kaidalov, V.A. Khoze, A.D. Martin and M.G. Ryskin, *Phys. Lett. B* **567**, 61 (2003).
16. H1 Collaboration, paper 987, submitted to the 31st *Int. Conf. on High Energy Physics* (ICHEP), Amsterdam (2002); paper 087, submitted to the *Int. Europhysics Conf. on High Energy Physics* (EPS), Aachen (2003); F.-P. Schilling, Proc. of this conference, *Eur. Phys. J. C* **33**, S530 (2004).
17. H. Jung, *Comp. Phys. Commun.* **86**, 147 (1995).
18. M. Klasen and G. Kramer, *Z. Phys. C* **72**, 107 (1996).
19. M. Klasen and G. Kramer, *Z. Phys. C* **76**, 67 (1997); M. Klasen, T. Kleinwort and G. Kramer, *Eur. Phys. J. direct C* **1**, 1 (1998).
20. M. Klasen and G. Kramer, Proc. of the 12th *Int. Workshop on Deep Inelastic Scattering* (DIS), D. Bruncko, J. Ferencei and P. Strizenec (eds.), Kosize, Inst. Exp. Phys. SAS, p. 492 (2004), hep-ph/0401202.
21. M. Klasen and G. Kramer, *Eur. Phys. J. C* **38**, 93 (2004).
22. S. Kagawa, Proc. of the 12th *Int. Workshop on Deep Inelastic Scattering* (DIS), D. Bruncko, J. Ferencei and P. Strizenec (eds.), Kosize, Inst. Exp. Phys. SAS, p. 482 (2004).
23. H1 Collaboration, C. Adloff et al., *Z. Phys. C* **76**, 613 (1997).
24. A. Bruni, M. Diehl and F.-P. Schilling, Proc. of the 12th *Int. Workshop on Deep Inelastic Scattering* (DIS), D. Bruncko, J. Ferencei and P. Strizenec (eds.), Kosize, Inst. Exp. Phys. SAS, p. 3 (2004).
25. H1 Collaboration, A. Aktas et al., *Eur. Phys. J. C* **51**, 549 (2007).
26. S. Frixione, *Nucl. Phys. B* **507**, 295 (1997).
27. ZEUS Collaboration, S. Chekanov et al., *Eur. Phys. J. C* **55**, 177 (2008).
28. H1 Collaboration, A. Aktas et al., *JHEP* **10**, 042 (2007).
29. S. Ellis and D. Soper, *Phys. Rev. D* **48**, 3160 (1993); S. Catani et al., *Nucl. Phys. B* **406**, 187 (1993).
30. M. Klasen and G. Kramer, *Phys. Lett. B* **366**, 385 (1996).
31. S. Frixione et al., *Phys. Lett. B* **319**, 3986 (1993).
32. M. Glück, E. Reya and A. Vogt, *Phys. Rev. D* **46**, 1973 (1992).
33. M. Klasen and G. Kramer, *J. Phys. G* **31**, 1 (2005).
34. M. Klasen, Proc. of the Workshop on *High-energy photon collisions at the LHC*, D. d'Enterria, M. Klasen and K. Piotrkowski (eds.), LPSC 08-054, arXiv:0806.0915 [hep-ph].